Journal of Materials Chemistry C

Accepted Manuscript

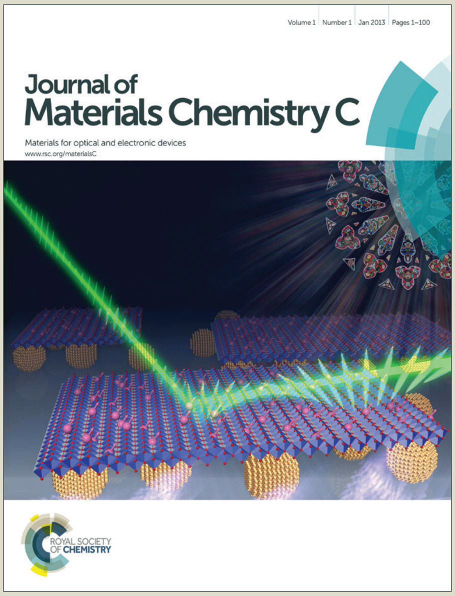

ROYAL SOCIETY OF CHEMISTRY

www.rsc.org/materialsC

Electronic structures of multilayer two-dimensional silicon carbide with oriented misalignment

Xiao Lin[1], Shisheng Lin[1,*], Yang Xu[1,*], and Hongsheng Chen[1,2,3*]

[1]*College of Information Science and Electronic Engineering,*
Zhejiang University, Hangzhou 310027, P. R. China.
[2]*State Key Laboratory of Modern Optical Instrumentation,*
Zhejiang University, Hangzhou 310027, P. R. China.
[3]*The Electromagnetics Academy at Zhejiang University,*
Zhejiang University, Hangzhou 310027, P. R. China.

[*]*Corresponding authors: shishenglin@zju.edu.cn (S.S. Lin), yangxu-isee@zju.edu.cn (Y. Xu),*
hansomchen@zju.edu.cn (H. S. Chen)

Abstract: The direct bandgap is favored for optoelectronic applications, such as light emitting or laser diodes and solar cells. While monolayer two-dimensional graphene-like silicon carbide (2d-SiC) possesses a moderate direct bandgap, multilayer 2d-SiC was recently found to exhibit an indirect bandgap. In this paper, our *ab initio* electronic study demonstrates that a controllable direct bandgap of bilayer/trilayer 2d-SiC can be realized via the interlayer oriented misalignment, where their direct-bandgap character can be maintained for most rotation angles. This misalignment-induced direct bandgap shows a decreasing tendency with a larger commensuration cell, where the minimum direct optical transition frequency can vary from infrared to visible. Our work implies that the interlayer oriented misalignment is a crucial way to tailor electronic structures of multilayer 2d-SiC, facilitating potential applications for optoelectronic devices.

Introduction

Two-dimensional graphene-like silicon carbide (2d-SiC) has emerged as an intriguing new class of layered nanostructure [1-10], due to its recent success in experimental fabrication [11]. While bulk SiC exists in either a sphalerite or wurtzite structure with an indirect bandgap [12], the monolayer 2d-SiC is reported to own a moderate direct bandgap of ~2.5 eV, which can be tuned via the in-plane strain [13-14], and shows improved photoluminescence capability [11]. Novel physics emerges by the stacking of two or more atomic layers. For example, in contrast to monolayer 2d-SiC, multilayer 2d-SiC is found to be sensitive to the layer thickness and possess an indirect-bandgap character [13], hindering their practical applications in optoelectronic devices such as light emitting diodes and solar cells. In practical samples, the neighboring layers for the layered systems are often arbitrarily aligned with respect to each other, leading to an interlayer oriented misalignment [15-21]. The complicated interactions induced by the oriented misalignment would distinctively change their pristine electronic and optical properties, which has been widely studied in graphene and its analogue systems, such as bilayer graphene [16-19], graphene/hexagonal boron nitride [20-21], and bilayer molybdenum disulfide (MoS_2) [15]. Understanding these interactions is important for building functional heterojunction devices and novel hybrid 2D materials. All of the above greatly motivate us to study the oriented misalignment in the multilayer 2d-SiC system, which has not been discussed yet. Here we investigate the influence of the oriented misalignment on the electronic structure of bilayer/trilayer 2d-SiC by using the *ab initio* calculations. The indirect-to-direct bandgap transition is for the first time found to be induced by the oriented misalignment, where the direct-bandgap character of multilayer 2d-SiC is maintained for most rotation angles. This newly revealed direct bandgap will decrease with a larger commensuration cell, varying between 1.2 eV and 2.1 eV.

Calculation methods

Before investigating the electronic structures of multilayer 2d-SiC with oriented misalignment, it is important to find the set of rotation angles which gives rise to the commensurate crystal structures. It is noted that the mathematical method to process this crystallographic problem is well developed in previous studies [22]. For the convenience of following expressions, here we will re-derive the calculations. The crystallographic problem is in fact to find appropriate rotations such that applied to the triangular lattice leave a subset of atoms coincident with the original unrotated lattice. We can express this condition as $\boldsymbol{a}_2 = \boldsymbol{R}\boldsymbol{a}_1$, where $\boldsymbol{a}_{1,2}$ and $\boldsymbol{R} = \begin{pmatrix} cos\theta & -sin\theta \\ sin\theta & cos\theta \end{pmatrix}$ are the direct-lattice vectors and the rotation operator, respectively, and θ is the rotation angle. With a standard choice of the basis vectors, this condition is equivalent to

$$\boldsymbol{T}\begin{pmatrix} m_1 \\ m_2 \end{pmatrix} = \boldsymbol{RT}\begin{pmatrix} n_1 \\ n_2 \end{pmatrix}, \tag{1}$$

where $\boldsymbol{T} = \begin{pmatrix} \sqrt{3} & \sqrt{3} \\ 1 & -1 \end{pmatrix}$ is the operator that transforms between the triangular lattice and Cartesian coordinate systems, and all components in vectors $\begin{pmatrix} m_1 \\ m_2 \end{pmatrix}$ and $\begin{pmatrix} n_1 \\ n_2 \end{pmatrix}$ are integer-valued. From Eq.(1), we have

$$\begin{pmatrix} m_1 \\ m_2 \end{pmatrix} = \begin{pmatrix} \frac{1}{\sqrt{3}} sin\theta + cos\theta & \frac{2}{\sqrt{3}} sin\theta \\ -\frac{2}{\sqrt{3}} sin\theta & -\frac{1}{\sqrt{3}} sin\theta + cos\theta \end{pmatrix} \begin{pmatrix} n_1 \\ n_2 \end{pmatrix}, \tag{2}$$

Eq. (2) is a Diophantine systems. A necessary condition for an integer solution of this Diophantine equation is that the matrix is rational-valued which implies that $sin\theta/\sqrt{3} = i_1/i_3$ and $cos\theta = i_2/i_3$, where $3i_1^2 + i_2^2 = i_3^2$, with $\{i_1, i_2, i_3\} \in \mathbb{Z}$ [22]. By solving the Diophantine equation, we have

$$i_3 m_1 = (i_1 + i_2)n_1 + 2i_1 n_2$$

$$i_3 m_2 = -2i_1 n_1 + (i_2 - i_1)n_2 \tag{3}$$

where $i_1 = p^2 - 2pq - 3q^2$, $i_2 = -(p^2 + 6pq - 3q^2)$, and $i_3 = 2(p^2 + 3q^2)$, with $\{p, q\} \in \mathbb{Z}$. It should be noted that for any (p, q) pair the Eq.(3) has infinitely many solutions which correspond to the same superlattices related by Eq.(1). Therefore, every commensuration of multilayer 2d-SiC can be labelled by a (p,q) integer pair [22]. From these equations, it is convenient to determine the primitive commensuration cells for these superlattices. In the following, we define $\delta = 3/\mathrm{gcd}(p,3)$ and $\gamma = \mathrm{gcd}(\mathrm{p}+3\mathrm{q}, \mathrm{p}-3\mathrm{q})$, where gcd is the abbreviation of the greatest common divisor. Then for the case of $\delta = 1$, we have

$$\boldsymbol{t}_1 = \frac{1}{\gamma}(p+3q)\boldsymbol{a}_1 + \frac{1}{\gamma}(p-3q)\boldsymbol{a}_2$$

$$\boldsymbol{t}_2 = -\frac{1}{\gamma}2p\boldsymbol{a}_1 + \frac{1}{\gamma}(p+3q)\boldsymbol{a}_2 \qquad (4)$$

and for the case of $\delta = 3$, we have

$$\boldsymbol{t}_1 = \frac{1}{\gamma}(p+q)\boldsymbol{a}_1 - \frac{1}{\gamma}2q\boldsymbol{a}_2$$

$$\boldsymbol{t}_2 = -\frac{1}{\gamma}(p-q)\boldsymbol{a}_1 + \frac{1}{\gamma}(p+q)\boldsymbol{a}_2 \qquad (5)$$

The vectors, $\boldsymbol{t}_1$ and $\boldsymbol{t}_2$, are the primitive vectors for these superlattices. From these primitive vectors, we can derive the rotation angle as $\theta = cos^{-1}(\frac{3q^2-p^2}{3q^2+p^2})$, where for $\mathrm{p} \leq \mathrm{q}$ we have $0 < \theta < \pi/3$. Note that every commensuration can also be labelled by the rotation angle due to its uniqueness. In this work, we treat the first two layers un-rotated (i.e. energetically stable AB stacking) and only rotate the third layer with respect to the second layer for the case of trilayer 2d-SiC. Then the total atom number in the commensuration cell in each layer is $\mathrm{N} = 6(3q^2+p^2)/(\delta\gamma^2)$. From above, the total atom number in the commensuration cell in each layer will rapidly increase when the rotation angle $\theta \rightarrow 0$, making the *ab initio* simulations rather unrealistic. Fortunately, there exists a range of rotation angles with a moderate atom number in the commensuration cell, which is suitable for our *ab initio* simulations. One example of bilayer 2d-SiC with $(\mathrm{p},\mathrm{q}) = (1,2)$ or a rotation angle of 32.2° is schematically depicted in Fig.1. The Moire's pattern for the bilayer system can be clearly seen, where the commensuration cell for the superlattice is denoted by the dashed lines in Fig.1.

The electronic structures of multilayer 2d-SiC are investigated through density functional theory (DFT) in the generalized gradient approximation (GGA) by using the commercial SIESTA codes [23], where the detailed setup for the *ab initio* simulations follows our previous works [13, 24]. The bond length of 2d-SiC is theoretically set to be 1.79 Å by energy optimization [13], consistent with the experimental value [11]. The exchange-correlation function of GGA is represented by the revised Perdew-Burke-Ernzerh (RPBE) approximation [25]. Double ζ polarized numerical atomic basis sets and norm-conserving pseudo-potentials are used. Already-standard corrections like LDA/GGA+U are mainly used to calculate redox reaction energies of many transition metal compounds with localized (or strongly correlated) *d* and *f* electrons, since the self-interaction error in LDA/GGA is not cancelled out in redox reactions where an electron is transferred between significantly different environments [26-28]. Here because we calculate the electronic properties of multilayer 2d-SiC without any metal oxides or localized *d* and *f* electrons, GGA is chosen here. We also note that the conventional DFT cannot treat the van der Waals (vdW) force effectively. This makes it difficult to obtain the precise interlayer distance in multilayer systems, leading to the underestimation of bandgaps [29-30]. We thus set the interlayer distance of neighboring 2d-SiC layers to be 3.47 Å from previous experiments [11]. The vdW density functional (vdW-DF) interaction calculation, on the other hand, employs a more accurate semilocal exchange functional and a large-*N* asymptote gradient correction in determining the vdW kernel [31-33]. The vdW-DF in the SIESTA-trunk-367 package is thus used here to take account of the polarization effect and improve the description of the nonlocal vdW interaction [31-33]. We set the electronic temperature to be 300 K. To avoid spurious interaction, a vacuum space (≥2.5 nm) between periodic images of the slabs is needed. A *k*-grid-Monkhorst-Pack mesh of 100 × 100 × 1 and a 300 Ry energy cutoff are set to ensure converged GGA results.

Results and discussions

To facilitate the *ab initio* simulations, we have exploited all the possible rotation angles with the total atom number in the commensuration cell in each layer smaller than 90. These rotation angles are $30^\circ \pm 30^\circ$, $30^\circ \pm 8.2^\circ$, $30^\circ \pm 2.2^\circ$, $30^\circ \pm 16.8^\circ$, $30^\circ \pm 12.1^\circ$, $30^\circ \pm 20.6^\circ$, $30^\circ \pm 14.8^\circ$, with the corresponding total atom number in the commensuration cell in each layer increasing from 2, 14, 26, 38, 62, 74, to 86, respectively. Note that the rotation angles of 60° and 0° are energetically stable AB stacking and energetically unstable AA' stacking, respectively.

The influence of the oriented misalignment on the electronic structure of bilayer 2d-SiC is shown in Figs.2-3. Fig.2 shows the evolution of the band structures of bilayer 2d-SiC with increasing atom number in the commensuration cell. When the atom number in the commensuration cell in each layer is $\mathrm{N} \leq 14$, bilayer 2d-SiC shows an indirect bandgap character, except for the energetically unstable AA' stacking. When further increasing the atom number in the commensuration cell, there are distinctive changes for the electronic structure. The band lines in the top of the valence band and the bottom of the conduction band become smoother with larger commensuration cell. Most notably, a direct bandgap character of bilayer 2d-SiC emerges and is maintained when the total atom number in the commensuration cell in each layer is $\mathrm{N} \geq 26$. Although we have only done simulations for limited cases due to our computing capability, we still can safely conclude from Fig.2 that the direct bandgap character will be preserved for cases with larger commensuration cells. We thus expect a direct bandgap character being found in most of the practical samples of bilayer 2d-SiC with oriented misalignment. It was previously shown that the oriented misalignment would effective decouple or weaken the interaction between two neighboring layers, such as twisted bilayer graphene [22]. In this respect of the bandgap character, we argue that most bilayer 2d-SiC with oriented misalignment more closely resembles two weakly perturbed monolayer direct bandgap 2d-SiC. Besides, although there is an indirect-to-direct bandgap transition when increasing the physical thickness both for 2d-SiC [13] and MoS_2 [34], the capability of indirect-to-direct bandgap transition induced by the oriented misalignment for the first time revealed here is unique for multilayer 2d-SiC, and is not applicable for multilayer MoS2 [15]. Our revealed direct bandgap character shall favor multilayer 2d-SiC in the potential optoelectronic applications.

Fig.3 shows the evolution of the bandgap as a function of the atom number in the commensuration cell in each layer. Here we define the bandgap value as the average value of these two bandgaps for bilayer 2d-SiC with different rotation angles but having the same atom number in the commensuration cell. From Fig.3, the bandgap shows a decreasing tendency with larger commensuration cells from 2.1 eV to 1.7 eV. Therefore, varying the interlayer rotation angle would result in strong tuning of the minimum direct optical transition energy. With the development of nanotechnology in 2D materials, such as artificially tailoring the rotation angle between neighboring atomic layers [15], our work indicates the oriented misalignment is a crucial way in tailoring the electronic properties of multilayer 2d-SiC.

To generalize our finding, we also investigate the influence of oriented misalignment in trilayer 2d-SiC, as shown in Figs. 3-4. Similar results are found. From Fig.3, we can safely argue that a direct bandgap for trilayer 2d-SiC can be maintained for most rotation angles with large commensuration cells. From Fig.4, the bandgap shows a decreasing tendency with larger commensuration cells from 1.8 eV to 1.2 eV. Since the capability of indirect-to-direct bandgap transition for bilayer/trilayer 2d-SiC is caused by the interlayer oriented misalignment, we argue that this capability should also be applicable for other multilayer 2d-SiC. It is noted that 2D materials are often used as donor materials, and 2D materials such as graphene or silicone with mediate bandgaps (i.e. 1.0-2.0 eV) that are highly desired by the field effect transistor and the solar cell [8,35] are still difficult to achieve. Therefore, our revealed mediate direct bandgap within the range of 1.2-2.1 eV obtained via the interlayer oriented misalignment shall be of scientific importance and desired by the industry.

Summary

To conclude, we explore the consequence of the interlayer rotation misalignment on the electronic structures of multilayer 2d-SiC. A novel physical phenomenon is revealed where the oriented misalignment can induce an indirect-to-direct bandgap transition for multilayer 2d-SiC. This induced direct bandgap, which decreases with a larger commensuration cell, is maintained for most rotation angles and controllable within the range of 1.2-2.1 eV through artificially tailoring the rotation angle between neighboring layers. Our results indicates that the oriented misalignment provides an efficient way to artificially tailor desirable electronic properties of multilayer 2d-SiC, which would favor their future optoelectronic applications such as light emitting diode, field effect transistor, and solar cells.

References

[1] R. Wu, K. Zhou, C. Y. Yue, J. Wei and Y. Pan, *Prog. Mater. Sci.*, 2015, **72**, 1-60.

[2] H. C. Hsueh, G. Y. Guo and S. G. Louie, *Phys. Rev. B*, 2011, **84**, 085404.

[3] H. Sahin, S. Cahangirov, M. Topsakal, E. Bekaroglu, E. Akturk, R. T. Senger and S. Ciraci, *Phys. Rev. B*, 2009, **80**, 155453.

[4] X. H. Sun, C. P. Li, W. K. Wong, N. B. Wong, C. S. Lee, S. T. Lee and B. K. Teo, *J. Am. Chem. Soc.*, 2002, **124**, 14464-14471.

[5] I. J. Wu and G. Y. Guo, *Phys. Rev. B*, 2007, **76**, 035343.

[6] L. Sun, Y. Li, Z. Li, Q. Li, Z. Zhou, Z. Chen, J. Yang and J. G. Hou, *J. Chem. Phys.*, 2008, **129**, 174114. .

[7] E. Bekaroglu, M. Topsakal, S. Cahangirov and S. Ciraci, *Phys. Rev. B*, 2010, **81**, 075433.

[8] L. J. Zhou, Y. F. Zhang and L. M. Wu, *Nano Lett.*, 2013, **13**, 5431-5436.

[9] C. Yang, Y. Xie, L. M. Liu and Y. Chena, *Phys. Chem. Chem. Phys.*, 2015, **17**, 11211-11216.

[10] P. Zhang, B. B. Xiao, X. L. Hou, Y. F. Zhu and Q. Jiang, *Sci. Rep.*, 2014, **4**, 3821.

[11] S. S. Lin, *J. Phys. Chem. C*, 2012, **116**, 3951-3955.

[12] P. A. Ivanov and V. E. Chelnokov, *Semicond. Sci. Technol.*, 1992, **7**, 863-880.

[13] X. Lin, S. Lin, Y. Xu, A. A. Hakro, T. Hasan, B. Zhang, B. Yu, J. Luo, E. Li and H. Chen, *J. Mater. Chem. C*, 2013, **1**, 2131-2135.

[14] T. Y. Lu, X. X. Liao, H. Q. Wang and J. C. Zheng, *J. Mater. Chem.*, 2012, **22**, 10062-10068.

[15] A. M. van der Zande, J. Kunstmann, A. Chernikov, D. A. Chenet, Y. You, X. Zhang, P. Y. Huang, T. C. Berkelbach, L. Wang, F. Zhang, M. S. Hybertsen, D. A. Muller, D. R. Reichman, T. F. Heinz and J. C. Hone, *Nano Lett*., 2014, **14**, 3869-3875.

[16] R. W. Havener, H. Zhuang, L. Brown, R. G. Hennig and J. Park, *Nano Lett*., 2012, **12**, 3162-3167.

[17] J. Hass, F. Varchon, J. E. Millan-Otoya, M. Sprinkle, N. Sharma, W. A. de Heer, C. Berger, P. N. First, L. Magaud and E. H. Conrad, *Phys. Rev. Lett.*, 2008, **100**, 125504.

[18] A. Luican, G. Li, A. Reina, J. Kong, R. R. Nair, K. S. Novoselov, A. K. Geim and E. Y. Andrei, *Phys. Rev. Lett.*, 2011, **106**, 126802.

[19] J. S. Alden, A. W. Tsen, P. Y. Huang, R. Hovden, L. Brown, J. Park, A. D. Muller and P. L. McEuen, *Proc. Natl. Acad. Sci. U.S.A.*, 2013, **110**, 11256-11260.

[20] C. R. Dean, L. Wang, P. Maher, C. Forsythe, F. Ghahari, Y. Gao, J. Katoch, M. Ishigami, P. Moon, M. Koshino, T. Taniguchi, K. Watanabe, K. L. Shepard, J. Hone and P. Kim, *Nature*, 2013, **497**, 598-602.

[21] B. Hunt, J. D. Sanchez-Yamagishi, A. F. Young, M. Yankowitz, B. J. LeRoy, K. Watanabe, T. Taniguchi, P. Moon, M. Koshino, P. Jarillo-Herrero, R. C. Ashoori, *Science*, 2013, **340**, 1427-1430.

[22] S. Shallcross, S. Sharma and O. A. Pankratov, *Phys. Rev. Lett.*, 2008, **101**, 056803.

[23] J. M. Soler, E. Artacho, J. D. Gale, A. Garcia, J. Junquera and P. Ordejon, *J. Phys. Condens. Matter*, 2002, **14**, 2745-2779.

[24] X. Lin, Y. Xu, A. A. Hakro, T. Hasan, R. Hao, B. Zhang and H. Chen, *J. Mater. Chem. C*, 2013, **1**, 1618-1627.

[25] B. Hammer, L. B. Hansen and J. K. Norskov, *Phys. Rev. B*, 1999, **59**, 7413.

[26] F. Zhou, M. Cococcioni, C. A. Marianetti, D. Morgan and G. Ceder, *Phys. Rev. B: Condens. Matter Mater. Phys.*, 2004, **70**, 235121.

[27] M. Cococcioni and S. de Gironcoli, *Phys. Rev. B: Condens. Matter Mater. Phys.*, 2005, **71**, 035105.

[28] L. Wang, T. Maxisch and G. Ceder, *Phys. Rev. B: Condens. Matter Mater. Phys.*, 2006, **73**, 195107.
[29] G. Giovannetti, P. A. Khomyakov, G. Brocks, P. J. Kelly and J. Brink, *Phys. Rev. B*, 2007, **76**, 073103.
[30] O. Leenaerts, H. Peelaers, A. D. Hernandez-Nieves, B. Partoens and F. M. Peeters, *Phys. Rev. B*, 2010, **82**, 195436.
[31] M. Dion, H. Rydberg, E. Schröder, D. C. Langreth and B. I. Lundqvist, *Phys. Rev. Lett.*, 2004, **92**, 246401.
[32] M. Birowska, K. Milowska and J.A. Majewski, *Acta Physica Polonica A*, 2011, **120**, 845-848.
[33] K. Lee, E. D. Murray, L. Kong, B. I. Lundqvist and D. C. Langreth, *Phys. Rev. B*, 2010, **82**, 081101.
[34] A. Splendiani, L. Sun, Y. B. Zhang, T. S. Li, J. Kim, C. Y. Chim, G. Galli and F. Wang, *Nano Lett.*, 2010, **10**, 1271-1275.
[35] A. Fleurence, R. Friedlein, T. Ozaki, H. Kawai, Y. Wang and Y. Y. Takamura, *Phys. Rev. Lett.*, 2012, **108**, 245501.

Acknowledgements

The authors would like to thank Shanghai Supercomputer Center for simulation support. This work was sponsored by the National Natural Science Foundation of China (No. 61322501, No. 61275183, No. 51202216, No. 61274123, and No. 61474099), the National Program for Special Support of Top-Notch Young Professionals, the Program for New Century Excellent Talents (NCET-12-0489) in University, the Fundamental Research Funds for the Central Universities (2014XZZX003-24), Special Foundation of Young Professor of Zhejiang University (No. 2013QNA5007), and the Zhejiang Provincial Natural Science Foundation (No. LR12F04001).

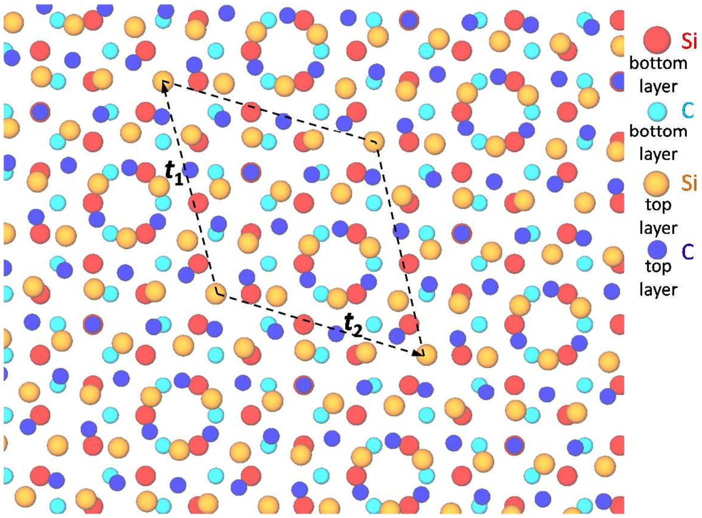

Fig. 1 Schematics of the atomic structure of bilayer 2d-SiC with oriented misalignment. The rotation angle is 32.2^o. The commensuration cell is marked by the dashed lines, with the primitive vectors for the super-lattice denoted as $\boldsymbol{t}_1$ and $\boldsymbol{t}_2$, respectively. The atom number in the commensuration cell in each layer is $\mathrm{N} = 26$.

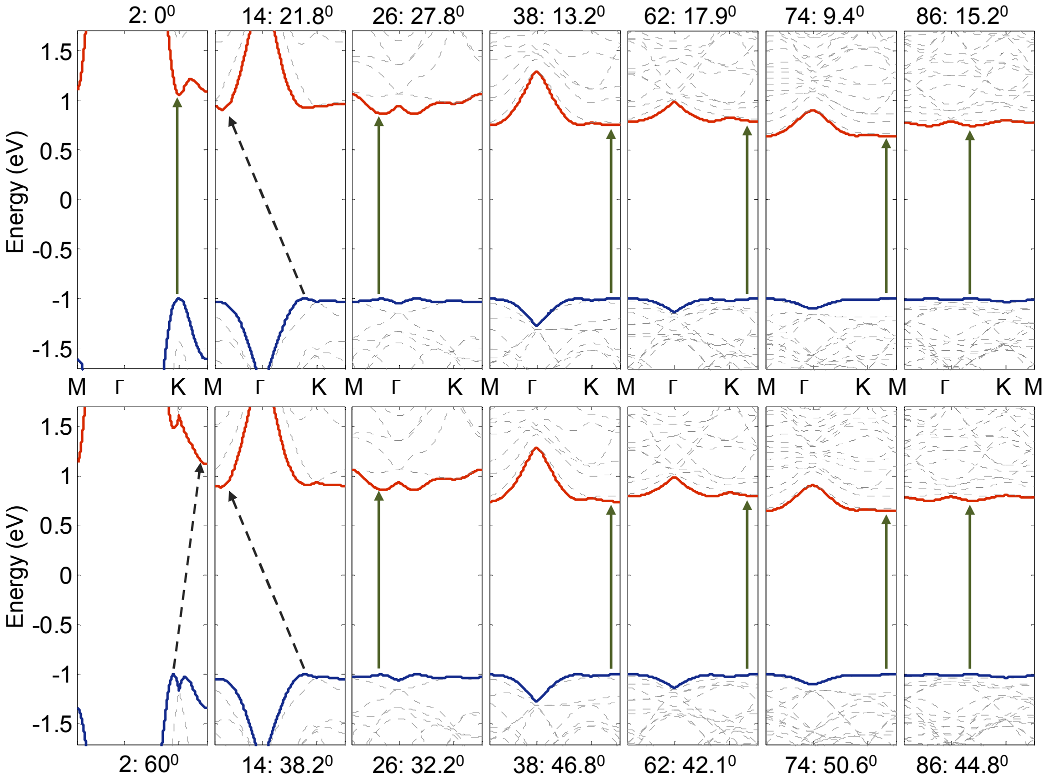

Fig. 2 Band structure evolution of bilayer 2d-SiC with oriented misalignment. The atom number in the commensuration cell in each layer (i.e. N, denoted in the left side of the colon) increases from left to right. The rotation angle is denoted in the right side of the colon. Bilayer 2d-SiC possesses a direct bandgap character for most rotation angles ($N \geq 26$).

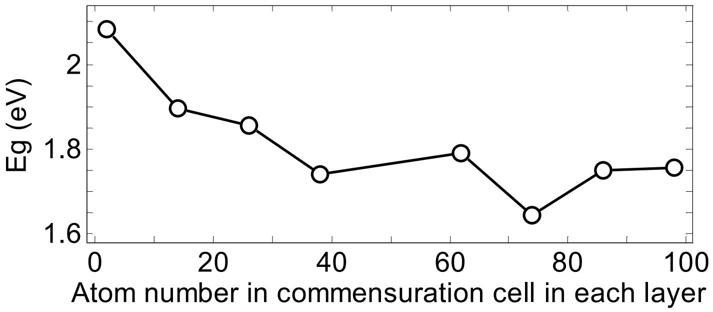

Fig. 3 Bandgap evolution of bilayer 2d-SiC with oriented misalignment as a function of the atom number in the commensuration cell in each layer. The bandgap value, i.e. E_g, is defined as the average value of these two bandgaps for bilayer 2d-SiC with the same atom number in the commensuration cell but having different rotation angles.

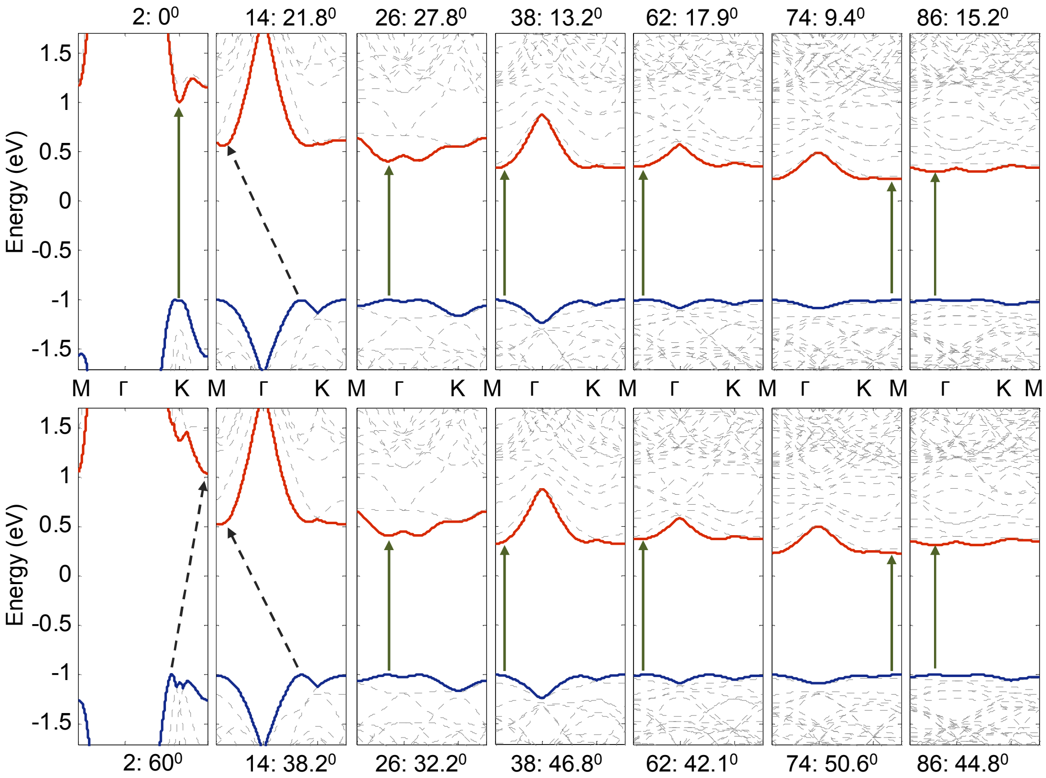

Fig. 4 Band structure evolution of trilayer 2d-SiC with oriented misalignment. The atom number in the commensuration cell in each layer (i.e. N, denoted in the left side of the colon) increases from left to right. The rotation angle is denoted in the right side of the colon. Trilayer 2d-SiC possesses a direct bandgap character for most rotation angles (N ≥ 26).

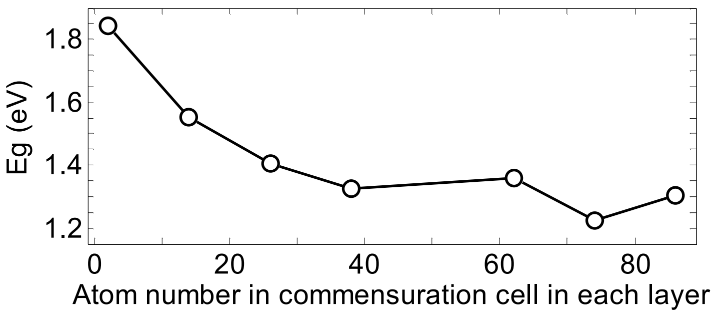

Fig. 5 Bandgap evolution of trilayer 2d-SiC with oriented misalignment as a function of the atom number in the commensuration cell in each layer. The bandgap value, i.e. E_g, is defined as the average value of these two bandgaps for trilayer 2d-SiC with the same atom number in the commensuration cell but having different rotation angles.

Graphical abstract

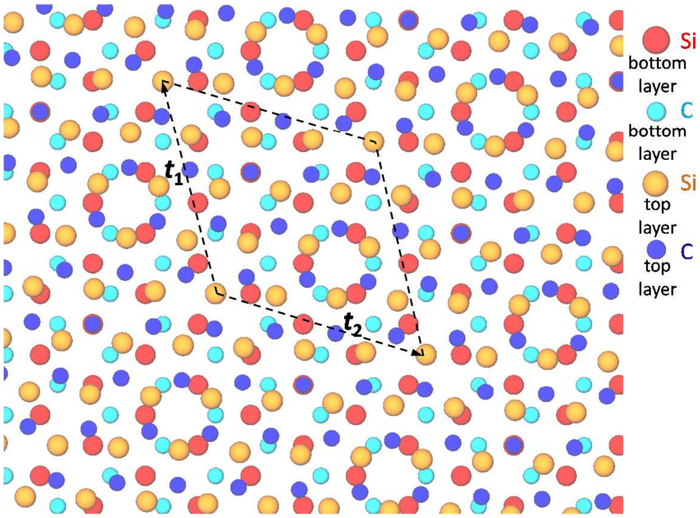

The direct bandgap is favored for optoelectronic applications, such as light emitting or laser diodes and solar cells. While monolayer two-dimensional graphene-like silicon carbide (2d-SiC) possesses a moderate direct bandgap, multilayer 2d-SiC was recently found to exhibit an indirect bandgap. In this paper, our *ab initio* electronic study demonstrates that a controllable direct bandgap of bilayer/trilayer 2d-SiC can be realized via the interlayer oriented misalignment, where their direct-bandgap character can be maintained for most rotation angles. This misalignment-induced direct bandgap shows a decreasing tendency with a larger commensuration cell, where the minimum direct optical transition frequency can vary from infrared to visible. Our work implies that the interlayer oriented misalignment is a crucial way to tailor electronic structures of multilayer 2d-SiC, facilitating potential applications for optoelectronic devices.